

Time-reversal symmetry breaking phase in the Hubbard model: A variational cluster approach study

Xiancong Lu,^{1,2} Liviu Chioncel,^{3,4} and Enrico Arrigoni²

¹*Department of Physics and Institute of Theoretical Physics and Astrophysics, Xiamen University, Xiamen 361005, China*

²*Institute of Theoretical and Computational Physics, Graz University of Technology, A-8010 Graz, Austria*

³*Augsburg Center for Innovative Technologies, University of Augsburg, D-86135 Augsburg, Germany*

⁴*Theoretical Physics III, Center for Electronic Correlations and Magnetism, Institute of Physics,*

University of Augsburg, D-86135 Augsburg, Germany

(Received 9 December 2011; published 19 March 2012)

We study the stability of the time-reversal symmetry breaking staggered-flux phase of a single band Hubbard model, within the variational cluster approach. For intermediate and small values of the interaction U , we find metastable solutions for the staggered-flux phase, with a maximum current per bond at $U \approx 3.2$. However, allowing for antiferromagnetic and superconducting long-range order it turns out that in the region at and close to half filling the antiferromagnetic phase is the most favorable energetically. The effect of nearest-neighbor interaction is also considered. Our results show that a negative nearest-neighbor interaction and finite doping favors the stability of the staggered-flux phase. We also present preliminary results for the three-band Hubbard model obtained with a restricted set of variational parameters. For this case, no spontaneous time-reversal symmetry breaking phase is found in our calculations.

DOI: [10.1103/PhysRevB.85.125117](https://doi.org/10.1103/PhysRevB.85.125117)

PACS number(s): 71.10.Fd, 71.27.+a, 71.10.Hf, 74.20.-z

I. INTRODUCTION

The Hubbard Hamiltonian is perhaps the simplest possible model to describe electronic interactions in solids. It is, however, difficult to solve and even after several decades of research there are still many open questions about its basic features. In particular, many competing phases have been proposed as candidates for the ground state in special parameter regions. The staggered-flux phase,^{1,2} known also as “orbital antiferromagnet,”³ was proposed to describe the ground state of Heisenberg antiferromagnetism. Many properties of the staggered-flux phase have been discussed in the past. However, less numerical evidence exists that supports the existence of this phase in the Hubbard or t - J model.⁴⁻¹⁰ The phenomena of pseudogap in cuprate superconductor contributed to the increased interest in the time-reversal symmetry broken phase. Chakravarty *et al.*¹¹ argued that the pseudogap region is due to the competition between d -wave superconductivity and d -density wave (DDW) state,^{12,13} which actually is the staggered-flux state breaking both time-reversal and translational symmetry. Based on the mean-field analysis of the three-band Hubbard model, Varma showed that a time-reversal symmetry breaking phase, the “circulating current phase,”¹⁴⁻¹⁷ is stable in some parameter regions. The orbital current of this phase is circulating along the O-Cu-O plaquette in each cell and thus, in contrast to DDW, translational symmetry is preserved. Motivated by this proposal, several theoretical and experimental groups have tried to find the signatures of orbital current in the CuO planes.¹⁸⁻²¹ However, no agreements have been obtained so far. A recent polarized neutron diffraction experiment shows that the spontaneous current occurs in loops involving apical oxygen orbitals.²² This picture is consistent with variational Monte Carlo (VMC) calculations,²³ although the authors observe that the computed current of the three-band Hubbard model is smaller for larger

system sizes; therefore computations on a larger system are required.

There has been much effort to search for the staggered-flux phase in the two-leg ladder, which is easier to study and can shed some light on the full two-dimensional lattices. By using the highly accurate density-matrix renormalization group technique, Marston *et al.*²⁴ and Schollwöck *et al.*²⁵ found evidence for the existence of a staggered-flux phase at and away from half filling, respectively. It has been shown that complex interactions are needed to stabilize this phase.^{24,25} Analytical studies using a bosonization/renormalization group (RG) method also found stable regions of this phase for weak interactions.²⁶⁻²⁹ In the present work we adopt the variational cluster approach (VCA) to study the time-reversal symmetry breaking phase. VCA allows one to evaluate the single-particle³⁰ and two-particle³¹ spectral functions, and to include symmetry breaking phases,^{30,32,33} such as antiferromagnetic and superconducting phases; therefore it can be easily extended to include the time-reversal symmetry breaking phase.

The paper is organized as follows. In Sec. II, we present the Hubbard Hamiltonian in a form that includes the single-particle parameters that are relevant for the time-reversal symmetry breaking. We review briefly the VCA method and introduce the coupling fields associated with the time-reversal symmetry breaking, so-called “Weiss” fields. These are the hopping Δt and its phase $\Delta\phi$, together with the current per bond which arises as a natural order parameter. The search for the spontaneous time-reversal breaking state within the interacting Hubbard model is presented in Sec. III. Sections III A and III B discuss the stability of the staggered-flux phase at and away from half filling for the single band Hubbard model. Our results indicate that the stable ground state for the interacting Hubbard model at half filling is the antiferromagnetic state. Away from half filling, the

competition with the superconducting phase is also investigated. Section III C discusses the effect of nearest-neighbor interaction on the staggered-flux phase. In Sec. III D, we extend the procedure described in Sec. II to the three-band Hubbard model and search for a spontaneous time-reversal symmetry breaking phase in this model. Finally, we draw our conclusions in Sec. IV.

II. HAMILTONIAN AND VARIATIONAL CLUSTER APPROACH

We consider the following two-dimensional (2D) Hubbard model on a square lattice:

$$H = - \sum_{\langle ij \rangle \sigma} (\tilde{t}_{ij} c_{i\sigma}^\dagger c_{j\sigma} + \text{H.c.}) + U \sum_i n_{i\uparrow} n_{i\downarrow}, \quad (1)$$

where $c_{i\sigma}^\dagger$ ($c_{i\sigma}$) creates (destroys) an electron on site i with spin σ , $n_{i\sigma} = c_{i\sigma}^\dagger c_{i\sigma}$ is the particle number operator, $\langle ij \rangle$ denotes nearest-neighbor sites, and U is the local Coulomb interaction. $\tilde{t}_{ij} = t e^{i\phi_{ij}}$ is the hopping-matrix element, where t is a real number and ϕ_{ij} is the phase factor on the bond $\langle ij \rangle$. In the following, we take $t = 1$ to be our unit of energy. If all $\phi_{ij} = 0$, Eq. (1) is the Hamiltonian of the standard Hubbard model with real hopping matrix. For $\phi_{ij} \neq 0$, Eq. (1) describes electrons hopping on lattices subjected to a magnetic field perpendicular to the plane of lattices provided the circulation of ϕ_{ij} is nonzero. For $\phi_{ij} = 0$ the Hamiltonian is symmetric under time reversal.

The VCA (Refs. 34 and 30) employed in this paper can be seen as an extension of cluster perturbation theory (CPT)^{35–37} based on the self-energy functional approach (SFA).^{38,39} One shortcoming of the CPT method is that it cannot study the spontaneous symmetry breaking phase. As an improvement over it, the VCA adds additional Weiss fields (describing a particular ordered state) to the cluster Hamiltonian, and optimizes the self-energy of the reference cluster by variational principle. The value for the variational parameter is determined by searching the saddle point of the SFA grand potential,

$$\Omega = \Omega' + \text{Tr} \ln (\mathbf{G}_0^{-1} - \Sigma)^{-1} - \text{Tr} \ln \mathbf{G}', \quad (2)$$

where \mathbf{G}_0 is the noninteracting Green's function, Ω' , Σ , and \mathbf{G}' are the grand-canonical potential, self-energy, and Green's function of the reference cluster, respectively. The system is in the ordered state if the corresponding Weiss field is nonzero at the saddle point of grand potential Ω .

For an initially time-reversal symmetric Hamiltonian ($\phi_{ij} = 0$), spontaneous symmetry breaking can occur under some circumstances. Within VCA this can be studied by introducing in the reference system an appropriate Weiss field.³⁰ The Weiss field (H'_{TR}) that breaks the time-reversal symmetry of the cluster Hamiltonian can be written in the following form:

$$H'_{\text{TR}} = \sum_{\langle ij \rangle \sigma} (\Delta t e^{i\Delta\phi_{ij}} c_{i\sigma}^\dagger c_{j\sigma} + \text{H.c.}). \quad (3)$$

Here, Δt is the amplitude of hopping acting as the strength of the Weiss field, and $\Delta\phi_{ij}$ is the phase factor on bond $\langle ij \rangle$ which determines the phase configuration of the time-reversal symmetry breaking phase. Both Δt and $\Delta\phi_{ij}$ should be treated as variational parameters when searching the saddle points of

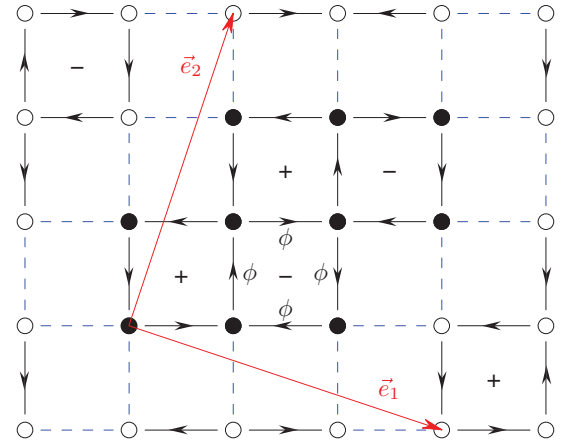


FIG. 1. (Color online) Staggered flux pattern in a 2D square lattice. ϕ is the phase on each bond in the direction indicated by the arrow. The total magnetic flux through a plaquette is 4ϕ . + and – denote the directions of the corresponding magnetic field. The black dots denote the ten-site reference cluster we use in our calculations. The vectors \vec{e}_1 and \vec{e}_2 are the translation vectors of VCA.

the SFA grand potential Ω in Eq. (2). A time-reversal symmetry breaking phase is characterized by a saddle point of Ω with nonzero values of both Δt and $\Delta\phi_{ij}$.

The natural order parameter for the time-reversal symmetry breaking phase is the current. For a typical bond $\langle lm \rangle$, the current is defined as

$$J_{lm} = \sum_{\sigma} i\tilde{t} (\langle c_{l\sigma}^\dagger c_{m\sigma} \rangle - \langle c_{m\sigma}^\dagger c_{l\sigma} \rangle). \quad (4)$$

It is obvious that J_{lm} is nonzero only if the time-reversal symmetry is broken. In the staggered-flux state the phase displays a pattern like the one illustrated in Fig. 1. If no other symmetries are broken one expects the absolute value of the phase to be the same on all bonds. We thus take $|\Delta\phi_{ij}| = \Delta\phi$ to be the same on all bonds.⁴⁰

Before proceeding to search for the spontaneous time-reversal symmetry breaking phase, we first test our code by introducing an external staggered-flux phase on a square lattice induced by an external magnetic field. The dynamics of two-dimensional lattice electrons coupled to an external magnetic field is described by the tight-binding Hamiltonian in Eq. (1), with the circulation of ϕ_{ij} on a given path being proportional to the magnetic flux through the enclosed surface.⁴¹

For a staggered-flux pattern and interaction $U = 0$, the model can be solved analytically and the energy spectrum obtained. The ground state E_G and current J can be computed by summing all the energies up to the Fermi energy and by the Hellmann-Feynman theorem. We carry out our test in the noninteracting limit for a staggered magnetic field with a phase pattern as shown in Fig. 1. All the quantities evaluated—spectral function, $E_G(\phi)$, and J —using our VCA code agree precisely with the analytical results.

For the case of interacting electrons we additionally checked the validity of the implementation by verifying thermodynamic consistency. Specifically concerning the current, its expectation values evaluated via the spectral function and via the Hellmann-Feynman theorem turn out to be identical.

Although this is obviously expected, in practice it is nontrivial since, as discussed in Ref. 42, this is only guaranteed if one uses the corresponding hoppings as variational parameters. By separating the hopping term in Hamiltonian (1) into real and imaginary parts, $\alpha(c_{i\sigma}^\dagger c_{j\sigma} + c_{j\sigma}^\dagger c_{i\sigma})$ and $i\beta(c_{i\sigma}^\dagger c_{j\sigma} - c_{j\sigma}^\dagger c_{i\sigma})$, with $\alpha = -t \cos(\phi)$ and $\beta = -t \sin(\phi)$, we confirm that treating β as a variational parameter the thermodynamic consistency condition discussed above is satisfied.

III. SPONTANEOUS STAGGERED-FLUX PHASE IN THE 2D HUBBARD MODEL

In this section, we study the stability of the spontaneous staggered-flux phase in the Hubbard model with *real* hopping matrix [i.e., $\phi_{ij} = 0$ in Eq. (1)]. The situation is different from what we discuss in Sec. II where the electrons are under an external staggered magnetic field. In order to allow for the time-reversal symmetry breaking order, we introduce a Weiss field H'_{TR} [cf. Eq. (3)] in the reference system. For the staggered-flux phase, the absolute value of the phase $|\Delta\phi_{ij}|$ is chosen to be equal for all bonds (i.e., $\Delta\phi$) and the staggering configuration is shown together with the VCA reference cluster in Fig. 1. In this paper, the reference cluster is solved by using exact diagonalization. We stress that it is important to choose a reference cluster with an even number of plaquettes, so that the net “magnetic field” in the cluster is zero.

A. Staggered-flux phase in the Hubbard model at half filling

In Fig. 2 we plot the difference between the values of the grand potential obtained when variational parameters are included relative to the cases when no variational parameters are considered. The results presented are for the case of half filling and different values of U . In the small U region (i.e., from 0 to 3.6), the values of the grand potential $\Omega(\Delta t, \Delta\phi)$ with both Δt and $\Delta\phi$ taken as variational parameters are *always* smaller than the grand potential $\Omega(\Delta t)$ with a sin-

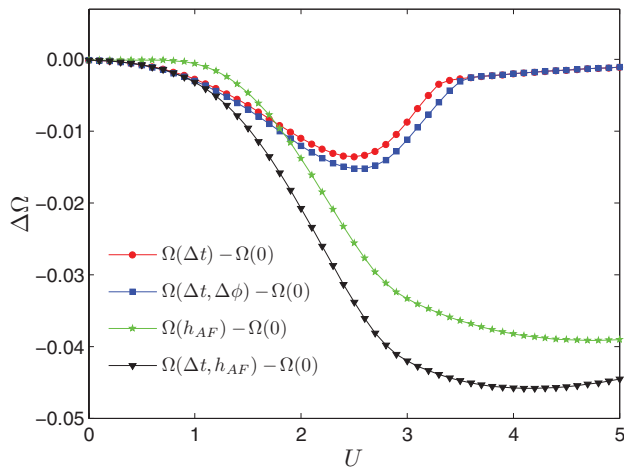


FIG. 2. (Color online) Difference between the grand potentials computed with variational parameters, such as the hopping Δt , phase factor $\Delta\phi$, and staggered magnetic field h_{AF} , with respect to the grand potential $\Omega(0)$ when no variational parameters are considered. The calculations are performed at half filling.

gle variational parameter Δt , the latter being also smaller than the grand potential obtained in a calculation with no variational parameters $\Omega(0)$. Accordingly, the staggered-flux phase is lower in energy than the correlated paramagnetic (nonmagnetic) state of the tight-binding Hamiltonian at half filling. At $U \approx 3.6$ the optimal $\Delta\phi$ vanishes indicating a phase transition to a phase without time-reversal symmetry breaking. This suggests that the staggered-flux phase is favored by small values of U . This situation was not considered within Ref. 1, which predicts that the staggered-flux phase is stable at large U limit, a consequence of the mean-field approach. At half filling one should expect that the ordered antiferromagnetic phase also plays an important role in the Hubbard model. In order to compare the stability of the flux phase with respect to the antiferromagnetic long-range order we included a Néel antiferromagnetic Weiss field

$$H'_{AF} = h_{AF} \sum_i (n_{i\uparrow} - n_{i\downarrow}) e^{i\mathbf{Q}\mathbf{r}_i} \quad (5)$$

into the reference system. Here, h_{AF} is the strength of a staggered magnetic field and $\mathbf{Q} = (\pi, \pi)$ is the antiferromagnetic wave vector. The calculations within the long-range ordered state shows that $\Omega(\Delta t, \Delta\phi)$ is larger than $\Omega(h_{AF})$ for values of $U > 1.9$, and is lower than $\Omega(h_{AF})$ when $U < 1.9$. But for a complete comparison, $\Omega(\Delta t, \Delta\phi)$ has to be compared with $\Omega(\Delta t, h_{AF})$ when both Δt and h_{AF} are treated as variational parameters in the long-range ordered state. As shown in Fig. 2, in this case $\Omega(\Delta t, \Delta\phi)$ is always larger than $\Omega(\Delta t, h_{AF})$ for the whole range of U .

Although our results indicate that the antiferromagnetic state is more stable than the staggered-flux phase for the half-filled 2D Hubbard model, the latter can be still considered as a metastable phase whose fluctuations affect the physics of the system, or which may become stable whenever antiferromagnetic long-range order is suppressed by some other mechanism.

In order to study the metastable staggered-flux state in more detail, we plot in Fig. 3(a) the difference in grand potentials $\Omega(\Delta t, \Delta\phi) - \Omega(\Delta t)$ (symbol \square , with labeling on the left) and the corresponding current J as a function of interaction U at half filling. The difference between the values of the grand potential increases with U , reaches a maximum for the value of $U \approx 3.2$, and then decreases to zero for $U \approx 3.6$. The largest difference between $\Omega(\Delta t, \Delta\phi)$ and $\Omega(\Delta t)$ is 0.0027, which corresponds to about 1 meV for $t \approx 500$ meV. The current per bond J (obtained in the staggered-flux phase) is computed by treating both Δt and $\Delta\phi$ as variational parameters. The computed values are shown in Fig. 3(a) with labeling on the right. One sees an opposite behavior of the current as a function of U with respect to $\Omega(\Delta t, \Delta\phi) - \Omega(\Delta t)$.

Figure 3(b) shows the values of variational parameters $\Delta\phi_{\text{sad}}$ and Δt_{sad} at the saddle points as a function of interaction U at half filling. One can see that the $\Delta\phi_{\text{sad}}$ increases as U is increasing in the small U region. After reaching its maximum around $U \approx 3.5$, where both the difference $\Omega(\Delta t, \Delta\phi) - \Omega(\Delta t)$ and the current J become zero, $\Delta\phi_{\text{sad}}$ drops sharply to zero. Note that, in the regions of $U < 0.7$ and $U \approx 3.5$, the difference between $\Omega(\Delta t, \Delta\phi)$ and $\Omega(\Delta t)$ is very small, in the same order as the accuracy of our calculation (1.0×10^{-4}). As in Fig. 3(b), the absolute value of variational

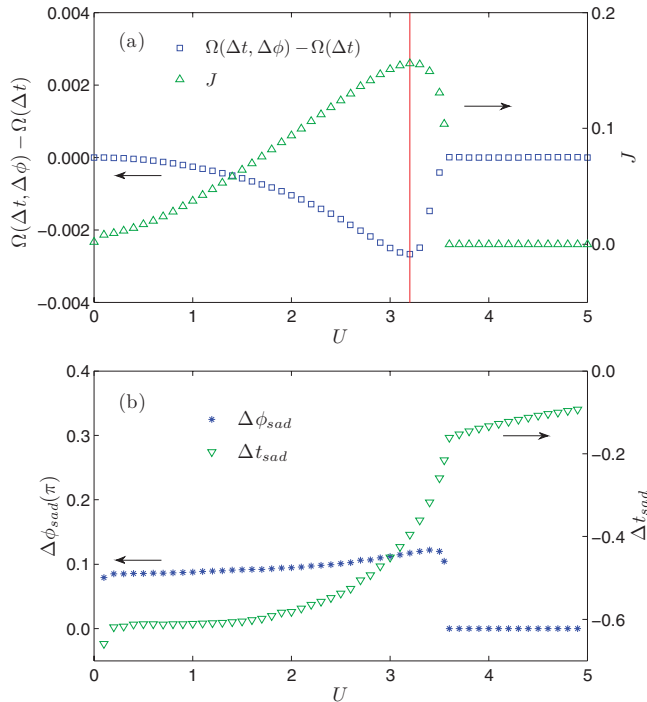


FIG. 3. (Color online) (a) The grand potential difference between $\Omega(\Delta t, \Delta \phi)$ and $\Omega(\Delta t)$ (denoted by \square with labeling on the left) and the current J corresponding to $\Omega(\Delta t, \Delta \phi)$ (denoted by Δ with labeling on the right) as a function of interaction U . (b) The value of variational parameters at the saddle points of $\Omega(\Delta t, \Delta \phi)$, $\Delta \phi_{\text{sad}}$ ($*$ with labeling on the left and in unit of π) and Δt_{sad} (∇ with labeling on the right), as a function of interaction U . The calculations are performed at half filling.

parameter Δt_{sad} is decreasing as U increases. The slope of the Δt_{sad} curve changes abruptly at the place where the value of $\Delta \phi_{\text{sad}}$ becomes zero.

B. Staggered-flux phase in the Hubbard model away from half filling

In this section, we study the stability of the staggered-flux phase when the system is away from half filling. We consider the competition between the staggered-flux phase, superconductivity, and antiferromagnetism. Away from half filling, the shift in the chemical potential $\Delta \mu$ must be treated as a variational parameter as well in order to satisfy the condition of thermodynamic consistency.³³ The d -wave superconducting phases^{30,32} can be described by introducing the corresponding Weiss field H'_{SC} :

$$H'_{\text{SC}} = h_{\text{SC}} \sum_{ij} \frac{\Delta_{ij}}{2} (c_{i\uparrow} c_{j\downarrow} + \text{H.c.}), \quad (6)$$

where h_{SC} is the strength of the nearest-neighbor d -wave pairing field and Δ_{ij} is the d -wave form factor.

Let us start by comparing the superconducting and staggered-flux states. In Fig. 4 we compare the grand potential of the superconducting phase $\Omega(\Delta \mu, \Delta t, h_{\text{SC}})$ with that of the staggered-flux phase $\Omega(\Delta \mu, \Delta t, \Delta \phi)$ for different values of the interaction parameter U . One can see that the values of the

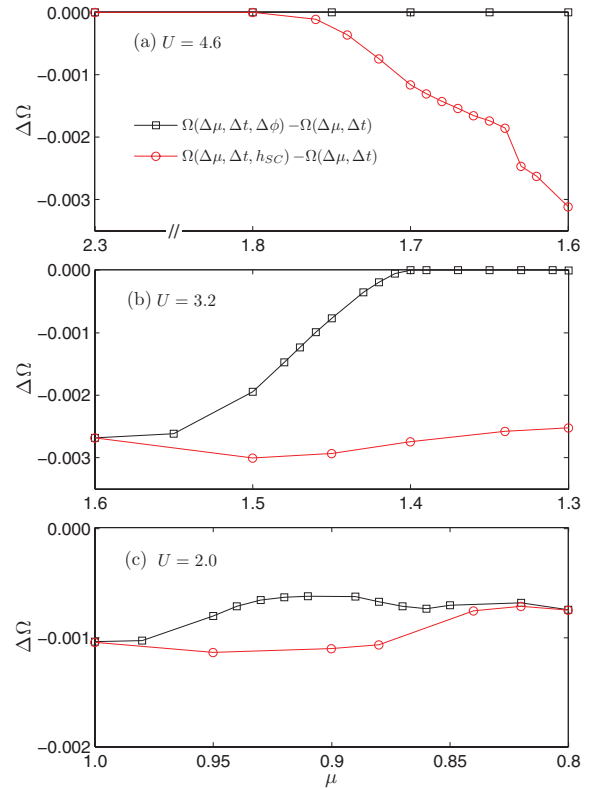


FIG. 4. (Color online) The grand potential of superconductor phase $\Omega(\Delta \mu, \Delta t, h_{\text{SC}})$ and staggered-flux phase $\Omega(\Delta \mu, \Delta t, \Delta \phi)$, with respect to $\Omega(\Delta \mu, \Delta t)$, as a function of chemical potential μ for various interactions U . $\Delta \mu$, Δt , $\Delta \phi$, and h_{SC} are variational parameters.

grand potential in the superconducting state $\Omega(\Delta \mu, \Delta t, h_{\text{SC}})$ and in the staggered-flux phase $\Omega(\Delta \mu, \Delta t, \Delta \phi)$ are equal at half filling. This can be easily understood because the d -wave pairing field H'_{SC} in Eq. (6) is connected to the staggered-flux field H'_{TR} in Eq. (3) by a particle-hole transformation at half filling.^{43,44} When away from half filling, $\Omega(\Delta \mu, \Delta t, h_{\text{SC}})$ is always *smaller* than $\Omega(\Delta \mu, \Delta t, \Delta \phi)$ for all interactions, implying that the superconducting state is more stable than the staggered-flux phase in this region. For the large U case ($U \gtrsim 4.0$), we cannot find a VCA saddle point corresponding to the staggered-flux phase neither at nor away from half filling. Here, the value of the variational parameter $\Delta \phi$ is always zero as seen in Fig. 4(a) for $U = 4.6$. Figure 4(a) shows that the values of the grand potential $\Omega(\Delta \mu, \Delta t, h_{\text{SC}})$ are smaller than that of $\Omega(\Delta \mu, \Delta t)$ and the difference between them is increasing as the chemical potential μ decreases. For smaller values of U a metastable VCA solution for the staggered-flux phase can be obtained; that is, $\Omega(\Delta \mu, \Delta t, \Delta \phi)$ is smaller than $\Omega(\Delta \mu, \Delta t)$ with a finite value of variational parameter $\Delta \phi$. For the intermediate U in Fig. 4(b), the staggered-flux phase disappears at some value of μ . Finally, for small U the metastable VCA solution for the staggered-flux phase always exists for the whole range of chemical potential, as seen in Fig. 4(c). Note that the plots in Fig. 4 are shown as a function of chemical potential, which corresponds to a doping in the range of 0–0.1.

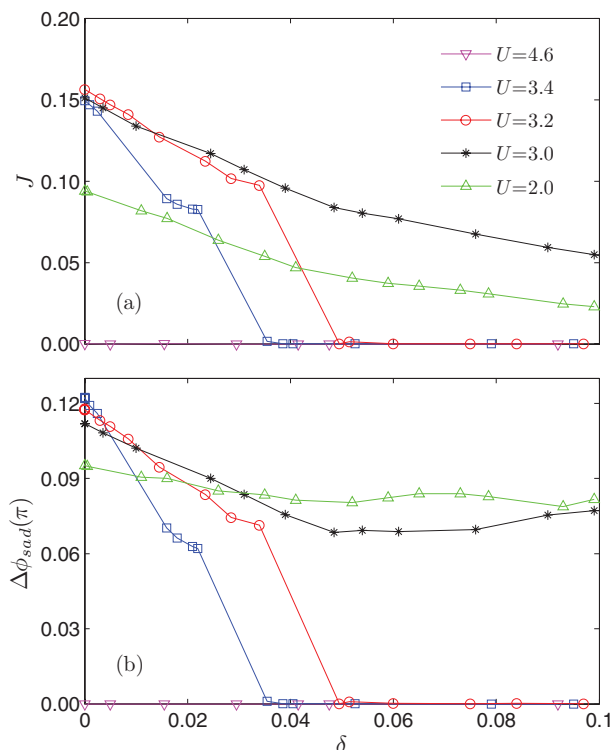


FIG. 5. (Color online) Current J (a) and the value of variational phase factor $\Delta\phi_{\text{sad}}$ (b) at the saddle points of $\Omega(\Delta\mu, \Delta t, \Delta\phi)$ as a function of doping δ for various interactions U .

In Fig. 5, the current J (a) and the value of variational phase factor $\Delta\phi_{\text{sad}}$ (b) at the saddle points of the staggered-flux phase are plotted as a function of doping δ for various interactions U . One can see that both J and $\Delta\phi_{\text{sad}}$ are zero for large $U \gtrsim 4.0$, indicating no VCA solution for the staggered-flux phase in this region. For intermediate U , J and $\Delta\phi_{\text{sad}}$ decrease as the doping δ is increasing and drop to zero at some value of doping (e.g., $\delta = 0.05$ for $U = 3.2$). For small U (e.g., $U = 2.0$), it seems that $\Delta\phi_{\text{sad}}$ remains as a finite value ($\sim 0.8\pi$) and does not drop to zero. However, the staggered-flux phase is less stable than the superconducting phase, as shown in Fig. 4.

Including the antiferromagnetic phase, we choose to look at the results for the values of $U = 3.2$, where the difference between $\Omega(\Delta t, \Delta\phi)$ and $\Omega(\Delta t)$ is maximal at half filling [see Fig. 3(a)]. In Fig. 6 we show the grand potential Ω with different variational parameters as a function of chemical potential μ . It is clear that $\Omega(\Delta\mu, \Delta t, h_{\text{AF}})$ is much smaller than both $\Omega(\Delta\mu, \Delta t, h_{\text{SC}})$ and $\Omega(\Delta\mu, \Delta t, \Delta\phi)$. Thus, the antiferromagnetic phase is the most stable state in this region of chemical potential. For even smaller chemical potential (or larger doping), the antiferromagnetic phase becomes unstable toward the superconducting phase.

In summary, we find that the staggered-flux phase is less stable than the superconducting state for all interactions and chemical potentials considered. For values of doping not very far away from half filling, the antiferromagnetic phase would be the most stable phase.

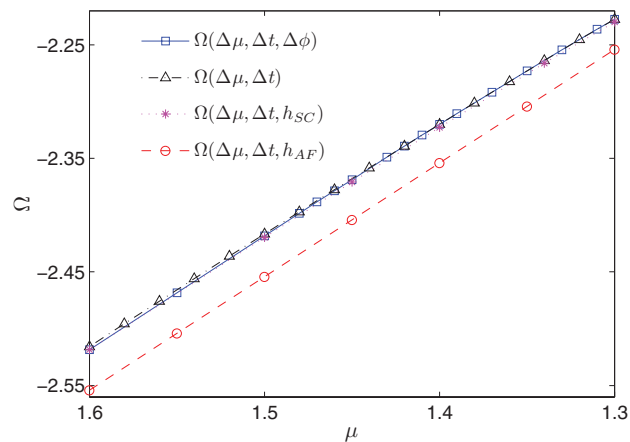


FIG. 6. (Color online) Grand potential Ω with different variational parameters ($\Delta\mu$, $\Delta\phi$, h_{SC} , and h_{AF}) as a function of the chemical potential μ for $U = 3.2$.

C. Staggered-flux phase in the Hubbard model with nearest-neighbor interaction

In this section, we discuss the effect of nearest-neighbor interaction on the staggered-flux phase in the Hubbard model. The nearest-neighbor interaction has the form $V \sum_{\langle ij \rangle} n_i n_j$, where $\langle ij \rangle$ denotes the nearest-neighbor pairs. This interaction can be added to the Hamiltonian of Eq. (1). In the following, we choose to look at the point with a fixed on-site interaction $U = 3.2$. In Fig. 7(a), the grand potential difference $\Delta\Omega = \Omega(\Delta t, \Delta\phi) - \Omega(\Delta t)$ is plotted as a function of nearest-neighbor interaction V at half filling. For a positive V , $\Delta\Omega$ is increasing to zero as V increases, implying that a positive repulsive V disfavors the staggered-flux phase. However, adding a negative V will decrease the value of $\Delta\Omega$. This means that an attractive nearest-neighbor interaction V is favorable for the formation of the staggered-flux phase. However, for negative V if $|V|$ is large enough (e.g., $V < -0.5$), there is no stable VCA solution anymore. The reason might be that a CDW order will form for very large attractive interaction and the staggered-flux phase is not stable anymore.

The effect of nearest-neighbor interaction V on the system away from half filling is shown in Figs. 7(b) and 7(c) for $V = 0.5$ and $V = -0.5$, respectively, where the $\Delta\Omega = \Omega(\Delta\mu, \Delta t, \Delta\phi) - \Omega(\Delta\mu, \Delta t)$ is plotted as a function of chemical potential μ . For positive $V = 0.5$, $\Delta\Omega$ increases slightly when μ deviates from the half-filling point $\mu = 3.6$ but is still inside the Mott gap region (i.e., $3.5 < \mu < 3.7$). $\Delta\Omega$ increases rapidly to zero as the doping (both particle and hole) becomes nonzero ($\mu < 3.5$ or $\mu > 3.7$). For negative $V = -0.5$, $\Delta\Omega$ remains nearly constant in the Mott gap region (i.e., $-0.425 < \mu < -0.375$). However, interestingly, it decreases as the system is doped (i.e., $\mu < -0.425$ or $\mu > -0.375$). Note that in both Figs. 7(b) and 7(c), the chemical potential corresponds to a density between 0.9 and 1.1. Here, we do not investigate the large doping region, in which a change of the particle sector in VCA is needed. Although the grand potential difference of the staggered-flux phase in Fig. 7(c) is decreasing with doping, it is still hard to compete with the antiferromagnetic phase. For example,

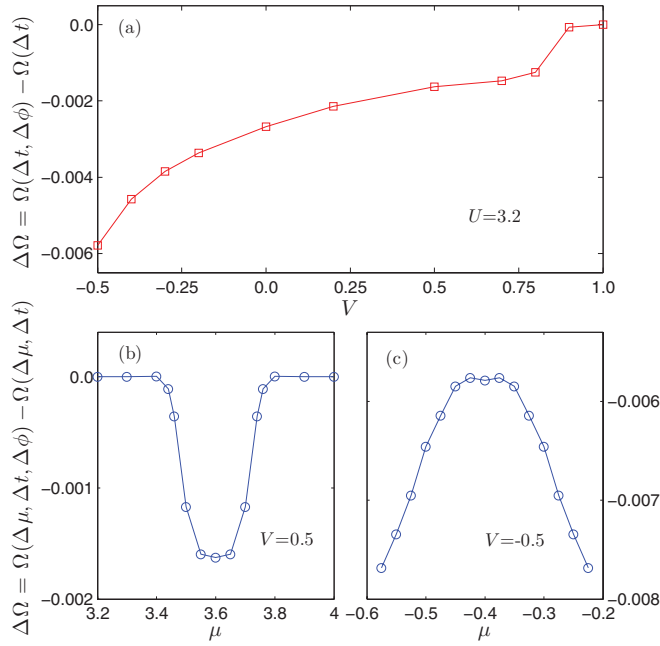


FIG. 7. (Color online) (a) The grand potential difference $\Omega(\Delta t, \Delta\phi) - \Omega(\Delta t)$ as a function of nearest-neighbor interaction V at half filling for a fixed on-site interaction $U = 3.2$. (b) and (c) show the grand potential difference $\Omega(\Delta\mu, \Delta t, \Delta\phi) - \Omega(\Delta\mu, \Delta t)$ as a function of chemical potential μ for nearest-neighbor interactions $V = 0.5$ and $V = -0.5$, respectively. The on-site interaction is also fixed at $U = 3.2$.

the grand potential difference of the antiferromagnetic phase, $\Omega(\Delta\mu, \Delta t, h_{AF}) - \Omega(\Delta\mu, \Delta t)$, is -0.0317 , which is much lower than that of the staggered-flux phase (-0.008) at the same point. Therefore, our calculation shows that a negative nearest-neighbor interaction and finite doping is energetically favorable for the formation of the staggered-flux phase.

D. Staggered-flux phase in the three-band Hubbard model

Our work can be naturally extended to consider the three-band Hubbard model to search for the existence of the spontaneous time-reversal symmetry breaking states. Such states are still under debate from both experimental and theoretical points of view. In the prototype realistic systems, the high- T_c cuprates, a crucial role is played by the CuO_2 planes, in which the oxygen orbitals are explicit degrees of freedom. The electron dynamics in the CuO_2 plane can be described by a minimal model, the three-band Hubbard model, containing the copper $d_{x^2-y^2}$ orbital and oxygen p_x and p_y orbitals. Experiments show evidence for time-reversal symmetry breaking in BSCCO with photoemission⁴⁵ and in $\text{HgBa}_2\text{CuO}_{4+\delta}$ with polarized neutron diffraction.²² However, no orbital currents are found in $\text{YBa}_2\text{Cu}_4\text{O}_8$ using Zeeman perturbed nuclear quadrupole resonance.⁴⁶ Early theoretical works discussed the flux phase in the single band model with current order and proposed it in connection to the pseudogap state in high- T_c cuprates.^{1,2,11} In order to stabilize the flux phase, Varma shows in a mean-field approach for the three-band model the necessity to go beyond on-site inter-

actions for an explicit treatment of the nearest-neighbor interactions between copper and oxygen.¹⁴⁻¹⁷ Although several theoretical calculations support Varma's picture,^{23,47} results of accurate numerical approaches, such as exact diagonalizations of small clusters^{18,19} and density-matrix renormalization group of ladders,⁴⁸ show that no spontaneous orbital currents are found in the three-band Hubbard model. Within this section we show some preliminary results of VCA calculations for the time-reversal symmetry breaking phase in the three-band Hubbard model.

The three-band Hubbard model under consideration is described by the Hamiltonian

$$\begin{aligned}
 H = & \sum_{(i,j)\sigma} t_{dp}^{ij} (d_{i\sigma}^\dagger p_{j\sigma} + \text{H.c.}) + \sum_{(j,k)\sigma} t_{pp}^{jk} (p_{j\sigma}^\dagger p_{k\sigma} + \text{H.c.}) \\
 & + U_d \sum_i n_{i\uparrow}^d n_{i\downarrow}^d + U_p \sum_j n_{j\uparrow}^p n_{j\downarrow}^p + V_{dp} \sum_{(i,j)\sigma} n_i^d n_j^p \\
 & + (\epsilon_d - \mu) \sum_{i\sigma} n_{i\sigma}^d + (\epsilon_p - \mu) \sum_{j\sigma} n_{j\sigma}^p. \quad (7)
 \end{aligned}$$

Here, $d_{i\sigma}^\dagger$ and $p_{j\sigma}^\dagger$ create a hole in copper $3d_{x^2-y^2}$ and oxygen $2p_\delta$ ($\delta = x, y$) orbitals, ϵ_d and ϵ_p are the on-site energy for copper and oxygen orbitals, μ is the chemical potential, t_{dp}^{ij} and t_{pp}^{jk} are the neighboring Cu-O and O-O hopping amplitudes. U_d , U_p , and V_{dp} are the Coulomb repulsions when two holes sit on the same copper orbital, the same oxygen orbital, or on the neighboring Cu and O orbitals. One difficulty associated with the study of the CuO_2 planes is the large number of parameters, giving rise to a huge phase space. Therefore, the choice of parameters for the three-band model of copper oxides has been extensively discussed in the literature.⁴⁹⁻⁵¹ Our choice corresponds to the following realistic value of parameters $t_{pp}^{jk} = 0.5$, $\Delta = \epsilon_p - \epsilon_d = 3.0$, $U_d = 8.0$, $U_p = 3.0$, and $V_{dp} = 0.5$, where we have taken the Cu-O hopping t_{dp}^{ij} as the unit of the energies.

In the inset of Fig. 8 we show the CuO_2 plane in which a 2×2 unit-cell plaquette is taken as the reference system for the VCA calculations. Thus, a plaquette contains four unit cells, each of them being composed of a Cu ($d_{x^2-y^2}$) and two O (p_x, p_y) sites. The implementation of time-reversal symmetry breaking within the three-band model follows the description given in Sec. II. In the present calculations we have used a reduced number of variational parameters, namely, the shift in the chemical potential $\Delta\mu$ as well as the shift $\Delta\phi$ of the phase on each hopping term, the latter having the form

$$\begin{aligned}
 H'_{\text{TR}} = & \sum_{(i,j)\sigma} t_{dp}^{ij} e^{i\Delta\phi_{dp\delta}} (d_{i\sigma}^\dagger p_{j\sigma} + \text{H.c.}) \\
 & + \sum_{(j,k)\sigma} t_{pp}^{jk} e^{i\Delta\phi_{pp}} (p_{j\sigma}^\dagger p_{k\sigma} + \text{H.c.}). \quad (8)
 \end{aligned}$$

$\Delta\phi_{dp\delta}$ ($\delta = x, y$) shifts the phases on the bonds between neighboring Cu-O atoms inside the 2×2 reference plaquette. Similarly, $\Delta\phi_{pp}$ shifts the phases on the bonds between neighboring O-O atoms within the same plaquette. Note that the magnitude of the shifts in the phases are not necessarily equal. In fact, we have performed the computations with four variational parameters: $\Delta\phi_{dp_x}$, $\Delta\phi_{dp_y}$, $\Delta\phi_{pp}$, and $\Delta\mu$. The direction and distribution of the phases on each hopping

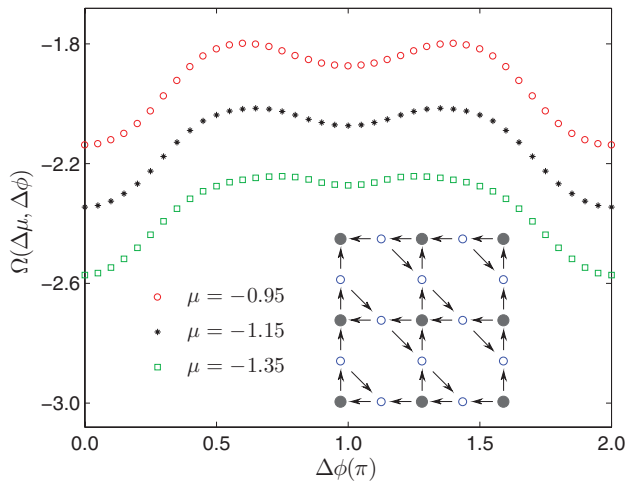


FIG. 8. (Color online) Grand potential $\Omega(\Delta\mu, \Delta\phi)$ of the three-band Hubbard model as a function of the values of variational parameter $\Delta\phi$. The inset shows the phase configuration used in the calculation.

bond are taken according to the “current pattern” proposed by Varma, Ref. 17. According to our calculations, none of the two current (phase) patterns considered in Varma’s mean-field proposal^{16,17} are stable. Within the calculations with four variational parameters the saddle point of grand potential Ω always locates at $\Delta\phi_{pp} = \Delta\phi_{dp_x} = \Delta\phi_{dp_y} = 0$. Therefore no spontaneous time-reversal symmetry breaking phases are found in our calculations.

In Fig. 8 we plot the grand potential $\Omega(\Delta\mu, \Delta\phi)$ as a function of $\Delta\phi$ for different values of μ . For the sake of illustration, the calculation has been performed using the simplifying assumption of equal phase shifts, i.e., when the values of $\Delta\phi_{pp}$, $\Delta\phi_{dp_x}$, and $\Delta\phi_{dp_y}$ are all equal. The phase (current) pattern is also shown in the inset of Fig. 8. This is the pattern denoted as the type Θ_{II} in the original work of Varma, Ref. 17. The saddle point in the grand potential Ω is obtained for zero phase on bonds, and turning on phase around zero will lead to an increase of Ω . The situation when all three $\Delta\phi$ are different is similar. Note that additional variational parameters such as Δt are required to complete our study on

the three-band Hubbard model; however, this is out of the scope of the present paper.

IV. CONCLUSION

The central aim of this paper was to extend the VCA method to study the time-reversal symmetry broken phase. We proposed to use two variational parameters, the hopping Δt and phase factor $\Delta\phi$, to study the staggered-flux phase in the 2D Hubbard model. Our calculation suggests a metastable staggered-flux phase in the intermediate and small U regions. For the case of half filling, the flux phase appears to be the most stable at $U \approx 3.2$. This implies that the staggered-flux phase, or at least its fluctuations, are more likely to be observed in the small U rather than in the large U region. We also studied the stability of the staggered-flux phase by comparing its grand potential with those of the superconductor and antiferromagnetic phases. We found that one of these latter phases is always more stable than the staggered-flux phase both at as well as away from half filling.

From our results on the one-band 2D Hubbard model we cannot draw a clear picture of which interactions are crucial to cause the orbital currents, although we clearly observe that a nearest-neighbor repulsion ($V > 0$) decreases the current that would be present in the absence of the intersite interaction. In contrast, an attractive nearest-neighbor interaction ($V < 0$) leads to an increase in the current in comparison with the $V = 0$ case. The staggered-flux order that emerges in the presence of $V < 0$ was previously reported within the strong-coupling regime.¹⁰ Our numerical results demonstrate that such a result is also applicable to the intermediate values of U . At last, we also extended the method for time-reversal symmetry breaking phase to study the three-band Hubbard model. By using only the shifts of phases on each hopping term as a variational parameter, we did not find a stable VCA saddle point for the staggered-flux phase.

ACKNOWLEDGMENTS

L.C. acknowledges discussions with P. Chakraborty and J. Kunes. X.L. thanks H. Allmaier, Z. B. Huang, and S. P. Kou for helpful discussions. This work was supported by the National Natural Science Foundation of China (Grants No. 11004164 and No. 10974163) and by the Austrian Science Fund (FWF) P18551-N16.

¹I. Affleck and J. B. Marston, *Phys. Rev. B* **37**, 3774 (1988).

²J. B. Marston and I. Affleck, *Phys. Rev. B* **39**, 11538 (1989).

³B. I. Halperin and T. M. Rice, *Solid State Phys.* **21**, 115 (1968).

⁴G. Kotliar and J. Liu, *Phys. Rev. B* **38**, 5142 (1988).

⁵P. Lederer, D. Poilblanc, and T. M. Rice, *Phys. Rev. Lett.* **63**, 1519 (1989).

⁶F. C. Zhang, *Phys. Rev. Lett.* **64**, 974 (1990).

⁷D. J. Scalapino, S. R. White, and I. Affleck, *Phys. Rev. B* **64**, 100506 (2001).

⁸A. Macridin, M. Jarrell, and T. Maier, *Phys. Rev. B* **70**, 113105 (2004).

⁹P. W. Leung, *Phys. Rev. B* **62**, 6112 (2000).

¹⁰T. D. Stanescu and P. Phillips, *Phys. Rev. B* **64**, 220509 (2001).

¹¹S. Chakravarty, R. B. Laughlin, D. K. Morr, and C. Nayak, *Phys. Rev. B* **63**, 094503 (2001).

¹²C. Nayak, *Phys. Rev. B* **62**, 4880 (2000).

¹³H. J. Schulz, *Phys. Rev. B* **39**, 2940 (1989).

¹⁴C. M. Varma, *Phys. Rev. B* **55**, 14554 (1997).

¹⁵C. M. Varma, *Phys. Rev. Lett.* **83**, 3538 (1999).

¹⁶M. E. Simon and C. M. Varma, *Phys. Rev. Lett.* **89**, 247003 (2002).

¹⁷C. M. Varma, *Phys. Rev. B* **73**, 155113 (2006).

¹⁸M. Greiter and R. Thomale, *Phys. Rev. Lett.* **99**, 027005 (2007).

- ¹⁹R. Thomale and M. Greiter, *Phys. Rev. B* **77**, 094511 (2008).
- ²⁰B. Fauque, Y. Sidis, V. Hinkov, S. Pailhes, C. T. Lin, X. Chaud, and P. Bourges, *Phys. Rev. Lett.* **96**, 197001 (2006).
- ²¹G. J. MacDougall, A. A. Aczel, J. P. Carlo, T. Ito, J. Rodriguez, P. L. Russo, Y. J. Uemura, S. Wakimoto, and G. M. Luke, *Phys. Rev. Lett.* **101**, 017001 (2008).
- ²²Y. Li, V. Balédent, N. Barisic, Y. Cho, B. Fauqué, Y. Sidis, G. Yu, X. Zhao, P. Bourges, and M. Greven, *Nature (London)* **455**, 372 (2008).
- ²³C. Weber, A. Läuchli, F. Mila, and T. Giamarchi, *Phys. Rev. Lett.* **102**, 017005 (2009).
- ²⁴J. B. Marston, J. O. Fjærestad, and A. Sudbø, *Phys. Rev. Lett.* **89**, 056404 (2002).
- ²⁵U. Schollwöck, S. Chakravarty, J. O. Fjærestad, J. B. Marston, and M. Troyer, *Phys. Rev. Lett.* **90**, 186401 (2003).
- ²⁶H. J. Schulz, *Phys. Rev. B* **53**, R2959 (1996).
- ²⁷E. Orignac and T. Giamarchi, *Phys. Rev. B* **56**, 7167 (1997).
- ²⁸J. O. Fjærestad and J. B. Marston, *Phys. Rev. B* **65**, 125106 (2002).
- ²⁹C. Wu, W. V. Liu, and E. Fradkin, *Phys. Rev. B* **68**, 115104 (2003).
- ³⁰C. Dahnken, M. Aichhorn, W. Hanke, E. Arrigoni, and M. Potthoff, *Phys. Rev. B* **70**, 245110 (2004).
- ³¹S. Brehm, E. Arrigoni, M. Aichhorn, and W. Hanke, *Europhys. Lett.* **89**, 27005 (2010).
- ³²D. Sénéchal, P. L. Lavertu, M. A. Marois, and A. M. S. Tremblay, *Phys. Rev. Lett.* **94**, 156404 (2005).
- ³³M. Aichhorn and E. Arrigoni, *Europhys. Lett.* **72**, 117 (2005).
- ³⁴M. Potthoff, M. Aichhorn, and C. Dahnken, *Phys. Rev. Lett.* **91**, 206402 (2003).
- ³⁵C. Gros and R. Valentí, *Phys. Rev. B* **48**, 418 (1993).
- ³⁶D. Sénéchal, D. Perez, and M. Pioro-Ladrière, *Phys. Rev. Lett.* **84**, 522 (2000).
- ³⁷S. G. Ovchinnikov and I. S. Sandalov, *Physica C* **161**, 607 (1989).
- ³⁸M. Potthoff, *Eur. Phys. J. B* **32**, 429 (2003).
- ³⁹M. Potthoff, *Eur. Phys. J. B* **36**, 335 (2003).
- ⁴⁰Due to the artificial symmetry breaking caused by the cluster partition, the order parameter is not uniform. Therefore, we obtain it as an average of the modulus of the current over all bonds *inside* the reference cluster.
- ⁴¹D. R. Hofstadter, *Phys. Rev. B* **14**, 2239 (1976).
- ⁴²M. Aichhorn, E. Arrigoni, M. Potthoff, and W. Hanke, *Phys. Rev. B* **74**, 024508 (2006).
- ⁴³P. A. Lee, N. Nagaosa, and X.-G. Wen, *Rev. Mod. Phys.* **78**, 17 (2006).
- ⁴⁴I. Affleck, Z. Zou, T. Hsu, and P. W. Anderson, *Phys. Rev. B* **38**, 745 (1988).
- ⁴⁵A. Kaminski, S. Rosenkranz, H. M. Fretwell, J. C. Campuzano, Z. Li, H. Raffy, W. G. Cullen, H. You, C. G. Olson, C. M. Varma, and H. Höchst, *Nature (London)* **416**, 610 (2002).
- ⁴⁶S. Strässle, B. Graneli, M. Mali, J. Roos, and H. Keller, *Phys. Rev. Lett.* **106**, 097003 (2011).
- ⁴⁷P. Chudzinski, M. Gabay, and T. Giamarchi, *Phys. Rev. B* **76**, 161101 (2007).
- ⁴⁸S. Nishimoto, E. Jeckelmann, and D. J. Scalapino, *Phys. Rev. B* **79**, 205115 (2009).
- ⁴⁹M. S. Hybertsen, M. Schlüter, and N. E. Christensen, *Phys. Rev. B* **39**, 9028 (1989).
- ⁵⁰A. K. McMahan, J. F. Annett, and R. M. Martin, *Phys. Rev. B* **42**, 6268 (1990).
- ⁵¹G. Dopf, A. Muramatsu, and W. Hanke, *Phys. Rev. Lett.* **68**, 353 (1992).